Design of a Rook shaped Microstrip Patch Antenna for WLAN Applications

Dr. G. Kalpanadevi[1], kalapanadevig.ece@krce.ac.in
Faculty, Department of ECE, K. Ramakrishnan College of Engineering, Tamil Nadu, India
Afshana R[2], Dharini N[3], Hima Shree S[4] and Hinduja KR[5]

Students, Department of ECE, K. Ramakrishnan College of Engineering, Tamil Nadu, India
afshana2721@gmail.com[2], krhinduja2005@gmail.com[5]

Abstract**—** This study presents the design and simulation of a rook-shaped microstrip patch antenna for 2.4 GHz Wireless Local Area Network (WLAN) applications. The proposed antenna is made from a FR-4 lossy substrate with a relative permittivity of 4.4, a loss tangent of 0.02, and a substrate thickness of 1.6 mm. The radiating patch is fashioned like a rook (castle) chess piece by carefully etching rectangular slots around the edge of a normal rectangular patch. This increases the current route length and enhances impedance matching. Both the radiating patch and the ground plane of the antenna are made of copper (annealed), and it employs edge feeding with a 50 microstrip feed line. The simulation results from the CST Studio Suite reveal a resonant frequency. Simulation results from CST Studio Suite reveal excellent impedance matching, with a resonance frequency of 2.409 GHz, a voltage standing wave ratio (VSWR) of 1.2583, and a return loss ($S_{1,1}$) of −18.831 dB. The radiation pattern exhibits a broadside radiation characteristic with a peak gain of −0.286 dBi. Its modest size and distinctive geometric shape make it an excellent fit for integration into modern WLAN-capable devices.

Index Terms - WLAN, 2.4 GHz, FR-4 substrate, rook-shaped antenna, radiation pattern, edge feed, return loss, VSWR, and microstrip patch antenna are among the index terms.

I. Introduction

The way people, gadgets, and infrastructure interact has changed dramatically in the last several decades due to the advancement of wireless communication. The antenna, a passive radiating component that launches and captures electromagnetic waves that transmit data over free space, is the central component of every wireless system. No matter how advanced the underlying electronics or signal processing algorithms are, no wireless link can be created without well-designed antennas. As a result, antennas are essential in almost every area of contemporary technology, including consumer electronics, cellular networks, broadband internet access, global navigation satellite systems, remote sensing platforms, and biomedical telemetry [1]. The ability of the antenna to effectively radiate power in desired directions, maintain stable impedance characteristics throughout the working band, and do so within the physical limitations set forth by the host device is directly related to the performance of a wireless system.

An ever-growing number of linked devices, each requiring dependable radio frequency links within strictly regulated frequency bands, characterizes modern wireless ecosystems. WLAN under IEEE 802.11b/g/n, Bluetooth, Zigbee, and several proprietary RF protocols used in smart home and industrial automation systems are among the short-range wireless connectivity technologies that rely on the 2.4 GHz ISM band, which is universally designated for unlicensed operation [2]. The sheer number of devices using this spectrum highlights how crucial it is to design antennas that not only precisely resonate at 2.4 GHz but also have well-controlled radiation characteristics, reducing interference with other systems while providing sufficient link margins for dependable data exchange. Antenna geometry, substrate selection, and feeding methodology must be carefully considered during the design phase in order to meet the demands of modern wireless ecosystems, which are characterized by an ever-increasing density of connected devices, each of which requires dependable radio frequency links.

The planar nature of microstrip patch antennas allows them to be deposited directly onto printed circuit boards using the same photolithographic processes used to manufacture the surrounding electronics, drastically reducing assembly complexity and unit cost [3]. Additionally, because they can be printed directly on the device's main board or on a dedicated RF layer, they add negligible thickness to the host device, which is a crucial advantage in the thin-profile consumer electronics market. As a result, this class of antenna is the standard for Wi-Fi modules, router cards, access point hardware, and embedded WLAN chipsets. However, there are well-known performance trade-offs associated with the rectangular and circular geometries that predominate in conventional microstrip antenna practice. These trade-offs include a narrow fractional bandwidth that limits tolerance to manufacturing variations and frequency drift, as well as gain figures that are limited by the electrical size of the patch relative to the operating wavelength [4].

A great deal of research has been focused on finding creative ways to change the patch geometry in order to get around these intrinsic restrictions. The distribution of surface currents across the radiating element is changed by adding cuts, slots, and notches to the patch. This changes the antenna's radiation behaviour, input impedance characteristics, and resonant frequencies [5]. In particular, it has been demonstrated that periodic boundary alterations can extend a patch's effective electrical length beyond its physical perimeter, allowing resonance at frequencies lower than those anticipated by traditional transmission line models for a patch with the same outside dimensions [6]. This electrical lengthening effect is highly advantageous when strict restrictions on the physical antenna footprint must be followed. Apart from slotted geometries, fractal patch boundaries created by repeated mathematical constructions have been studied as a means of achieving both multiband functioning and size reduction simultaneously [7]. Stacked patch topologies, which divide many resonant layers with thin dielectric spacers, have been utilised to increase the impedance bandwidth at the expense of a greater antenna height [8]. Choosing one of these methods, which all involve deliberate trade-offs between bandwidth, gain, size, fabrication complexity, and cost, requires careful evaluation of the specific requirements of the desired application.

As an alternative design philosophy that combines structural innovation with functional electromagnetic performance, geometrically unique patch shapes have garnered increasing attention. Recent literature has documented patches modelled after alphabetic characters, natural organisms, symbolic icons, and cultural artefacts, showing that non-traditional boundary shapes can generate beneficial radiation characteristics while also setting the design apart from commercial antenna solutions [9]. One of the six-piece chess pieces, the rook, offers an attractive geometric model for antenna construction. Its distinctive battlement pattern, which is typical of mediaeval castle towers, is formed by a solid central body from which a number of uniform rectangular projections stretch upward along the top edge.

The boundary that results from extending this profile to all four sides of a square radiating patch introduces a regular series of rectangular indentations that together lengthen the total perimeter current path, redistribute the surface current density throughout the patch, and alter the fringing field configuration at the radiating edges [10]. Together, these electromagnetic effects of the rook boundary cause the patch's fundamental resonance to shift toward a lower frequency than that of a simple rectangular patch with the same outer dimensions. This effectively provides a degree of electrical miniaturisation without the need for lumped loading elements or high-permittivity substrates.

The microstrip transmission line makes direct physical contact with the radiating patch's lateral edge as part of the edge feed feeding mechanism used for the suggested antenna. With no additional ground plane apertures, via-hole connections, or multilayer transitions needed, this method is one of the most straightforward feeds designs available to the antenna designer [11]. By placing the feed line at a suitable location along the patch edge where the input impedance of the resonant patch equals the characteristic impedance of the line, impedance matching to the standard 50 reference impedance is accomplished. Edge feeding is especially appealing for low-cost fabrication environments where process complexity needs to be kept to a minimum due to its simplicity. In order to accurately represent the metallic layers deposited or laminated during standard PCB manufacturing, the conducting elements of the antenna—the radiating patch and the ground plane—are given the material properties of annealed copper, which has an electrical conductivity of 5.8×10^2 S/m [12].

The glass-reinforced epoxy laminate FR-4 lossy, which has a loss tangent of 0.02 at microwave frequencies and a relative permittivity of 4.4, serves as the substrate for the antenna. Because of its established supply chain availability, dimensional stability, and mechanical resilience, FR-4 is one of the most popular PCB materials in the electronics industry [13]. Higher-performance microwave substrates, like Rogers RT/duroid, provide more precisely regulated permittivity values and reduced dielectric losses, but their substantially higher material costs may be unaffordable for consumer-grade wireless products. Instead of presenting optimistic results obtained under idealised material assumptions, the current work makes sure that the predicted antenna performance reflects the losses and permittivity variations that would be encountered in an actual low-cost fabrication run by purposefully choosing FR-4 as the simulation substrate [14]. CST Studio Suite, a full-wave electromagnetic solver that uses the Finite Integration Technique to precisely resolve the spatial and temporal development of electromagnetic fields within and around the antenna structure, is used to model and characterise the entire antenna structure [15].

The suggested rook-shaped antenna's computed performance shows resonance at 2.409 GHz with a return loss of −18.831 dB, a VSWR of 1.2583, and a broadside radiation pattern with a peak gain of −0.286 dBi. Together, these findings verify that the antenna satisfies the basic electrical specifications needed for WLAN operation in the 2.4 GHz band [16]. The suggested design is easily adaptable to physical prototype production using normal PCB procedures because of the rook shape's geometric simplicity, the use of commonly available materials, and a simple feeding system. A generalisable methodology for adapting patch geometries inspired by chess pieces to additional frequency bands and wireless standards is also provided by the design approach presented in this study [17].

This is how the paper is organised. The entire antenna design process is covered in detail in Section II, including the analytical formulation used for initial patch sizing, the parameterisation of the rook shape, substrate and conductor parameters, and feed line dimensioning. The complete set of simulated findings is shown in Section III, together with a thorough explanation of the radiation pattern characteristics, VSWR behaviour, and S-parameter response. The study's findings are collected in Section IV, which also suggests future directions for the research.

II. Antenna Design Methodology

A. Substrate Selection and Specifications

The choice of dielectric substrate is the cornerstone of any microstrip patch antenna design since it directly controls the radiating patch's effective permittivity, the feed line's characteristic impedance, the antenna's physical dimensions, and the total dielectric loss added to the system. FR-4 lossy is chosen as the substrate material in the suggested design. The PCB industry makes extensive use of FR-4, a glass-reinforced epoxy laminate, because of its superior mechanical qualities, dimensional stability under a range of thermal conditions, and substantially reduced procurement cost as compared to specialist microwave substrates. At microwave frequencies, FR-4's dielectric characteristics are defined by a loss tangent ($\tan \delta$) of 0.02 and a relative permittivity (ε_r) of 4.4. The most widely used standard laminate thickness in commercial PCB fabrication is represented by the substrate thickness (h), which is set at
1.6 mm. In accordance with the one-ounce copper cladding standard used in PCB manufacturing, the conducting layers—which include the ground plane on the bottom surface and the radiating patch on the top surface—are modeled as annealed copper with a thickness of 0.035 mm and an electrical conductivity of 5.8×10^2 S/m. Table I provides a summary of all substrate and conductor specifications.

The rook-shaped radiating patch installed on the FR-4 substrate with the ground plane positioned on the bottom surface is clearly shown in Fig. 1, the three-dimensional picture of the suggested antenna configuration as modelled in CST Studio Suite. The picture clearly shows the patch's battlement-like notched border, which depicts the general geometric profile of the

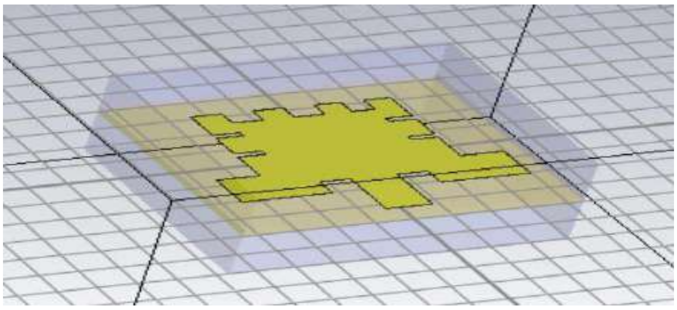

Fig. 1 3D view of the proposed antenna

Fig. 1. The rook-shaped copper radiating patch on the top surface of the FR-4 lossy substrate and the entire copper ground plane on the bottom surface are depicted in this three-dimensional model of the suggested rook-shaped microstrip patch antenna created in CST Studio Suite.

TABLE I: Substrate and Conductor Specifications

Parameter	**Value**
Substrate Material	FR-4 Lossy
Relative Permittivity (ε_r)	4.4
Loss Tangent ($\tan \delta$)	0.02
Substrate Thickness (h)	1.6 mm
Conductor Material	Copper (Annealed)
Conductor Conductivity (σ)	5.8×10^7 S/m
Conductor Thickness (t)	0.035 mm
Operating Frequency (f)	2.4 GHz

B. Initial Patch Dimension Calculation

The analytical computation of a traditional rectangular patch that resonates at the intended frequency of 2.4 GHz serves as the foundation for the rook-shaped patch design. The width and length of a rectangular microstrip patch antenna can be found using a well-known set of closed-form formulas provided by the standard transmission line model. The rook geometry is then built and parameterized using these formulas as the baseline dimensions.

The following formula, which strikes a compromise between radiation efficiency and avoiding higher-order mode excitation, is used to calculate the width of the radiating patch (W):

$$W = \frac{c}{2f_r}\sqrt{\frac{2}{\varepsilon_r + 1}}$$

where f_r is the resonant frequency (2.4 GHz), ε_r is the substrate's relative permittivity, and c is the speed of light in empty space (3×10^1 m/s). The fringing fields that extend past the patch's physical boundary into the surrounding air medium are taken into account by the effective permittivity (ε_{re}ff), which is determined by:

$$\varepsilon_{reff} = \frac{\varepsilon_r + 1}{2} + \frac{\varepsilon_r - 1}{2}\left(1+12\frac{h}{W}\right)^{-1/2}$$

Additionally, the patch's electrical length seems longer than its physical length due to the fringing effect. The expression for this length (ΔL) extension on each side of the patch is:

$$\Delta L = 0.412h\frac{(\varepsilon_{reff} + 0.3)\left(\frac{W}{h}+0.264\right)}{(\varepsilon_{reff} - 0.258)\left(\frac{W}{h}+0.8\right)}$$

The resonant frequency and the patch's effective length ($L_e$ff) are connected by:

$$L_{eff} = \frac{c}{2f_r\sqrt{\varepsilon_{reff}}}$$

The length extensions from both radiating edges are then subtracted to determine the patch's actual physical length (L):

$$L = L_{eff} - 2\Delta L$$

The initial rectangular patch dimensions, which act as the geometric reference for building the rook-shaped boundary, are obtained by substituting the known parameters, f_r = 2.4 GHz, ε_r = 4.4, and h = 1.6 mm, into the preceding formulae. Table II lists the calculated antenna dimensions.

C. Feed Line Design

The suggested antenna uses an edge feeding arrangement where a microstrip transmission line comes into direct touch with the patch's radiating edge. In order to ensure compatibility with common RF test equipment and system interfaces, the width of the microstrip feed line (Wf) is determined to present a characteristic impedance of 50 Ω. The following formulas, which are developed from the microstrip transmission line model, are used to calculate the feed line width.

For W/h > 2:

$$Z_0 = \frac{120\pi}{\sqrt{\varepsilon_{reff}}\left[\frac{W}{h} + 1.393 + 0.667\ln\left(\frac{W}{h}+1.444\right)\right]}$$

To maintain symmetric current distribution over the radiating aperture and excite the dominant TM_1^1 mode, the feed line is placed at the middle of the patch's non-radiating edge. In order to have the best impedance match at the resonant frequency, the feed line's length is tuned during simulation. In this design, the feed line connects directly to the patch edge, depending on the natural input impedance at the patch border for impedance matching, rather than using the inset depth. The feed line width of 3.06 mm, which was determined using the transmission line impedance formula and confirmed through parametric simulation in CST Studio Suite, is equivalent to the typical 50 Ω line width for the specified substrate parameters.

D. Rook-Shaped Patch Geometry

The unique feature of the proposed antenna is the rook-shaped boundary of the radiating patch, which is created by methodically adding uniform rectangular notches along all four sides of the baseline rectangular patch. This geometric modification is inspired by the chess rook piece's silhouette, which is characterized by a series of rectangular battlements projecting from the top of a solid tower body. When this battlement pattern is symmetrically replicated on all four sides of the patch, the resulting shape acquires the appearance of a rook when viewed from above, thereby achieving both aesthetically pleasing profile and a functionally modified electromagnetic boundary.

Surface currents that would normally flow straight across the patch edge are forced to avoid the notch borders because each notch added to the patch boundary eliminates a rectangular portion of conducting material from the patch's edge. The resonant surface currents' overall travel length is effectively increased by this detour, which is electromagnetically comparable to running a physically bigger patch at the same frequency. Consequently, the rook-shaped patch achieves a target resonance frequency with a smaller outer footprint than a traditional rectangular design, or it resonates at a lower frequency than a simple rectangular patch with the same outer dimensions.

In order to properly locate the resonant frequency at 2.4 GHz while preserving a symmetric current distribution that supports a well-formed broadside radiation pattern, the notch dimensions and their spatial arrangement along the patch perimeter are meticulously specified. To maintain the periodic nature of the rook geometry, the notches' breadth and depth remain consistent, and the distance between neighboring notches is likewise kept constant. The patch's bottom border is altered to make room for the feed line. The 50 Ω microstrip line extends downward toward the discrete port from the middle area of the bottom side, which is set up as the feed stub connection point.

Fig. 2 shows an annotated top-view schematic of the radiating element with all important geometric characteristics clearly labeled, along with the precise dimensions of the rook-shaped patch as taken from the CST Studio Suite simulation model. The figure shows how the rectangular notches are symmetrically arranged along the patch's top and side edges, how the bottom edge is set up to accommodate the feed line connection, and the exact millimeter-level measurements that control each notch's width, depth, inter-notch spacing, and lateral wing extension. Together, Figs. 1 and 2 offer a comprehensive geometric description of the suggested antenna, communicating the two-dimensional dimensional detail required for precise design replication as well as the three-dimensional physical structure. Table III provides a summary of the rook-shaped patch's primary geometric properties.

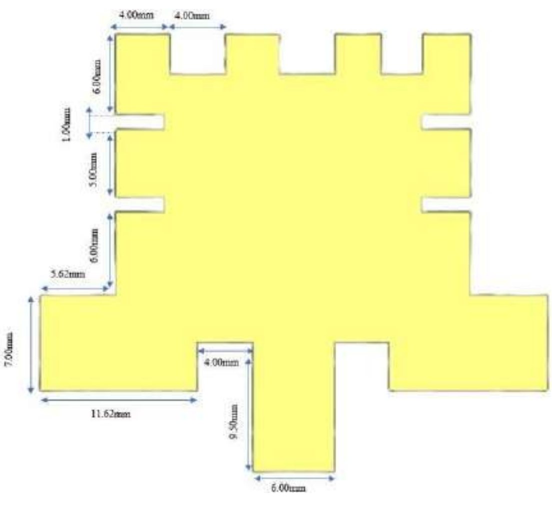

Fig. 2 Top view of the patch with dimensions

Fig. 2**.** shows the top view of the rook-shaped radiating patch with full dimensional annotations, showing the bottom feed connection area, the lateral wing extensions, and the periodic rectangular notch arrangement along all four sides.

TABLE III: Rook-Shaped Patch Geometric Parameters

Parameter	Description	Value
Notch Width (top)	Width of each rectangular notch	4.00 mm
Notch Spacing	Gap between adjacent notches	4.00 mm
Notch Depth 1	Depth of upper-row notches	6.00 mm
Notch Depth 2	Depth of middle-row notches	5.00 mm
Notch Separation	Vertical gap between notch rows	1.00 mm
Side Notch Depth	Depth of side boundary notches	6.00 mm
Side Extension	Horizontal protrusion at lower sides	5.62 mm
Lower Tab Width	Feed-side central tab width	4.00 mm
Lower Tab Length	Feed-side central tab length	9.50 mm
Feed Tab Base Width	Base width of feed tab	6.00 mm
Lateral Extension	Horizontal extent of lower wings	11.62 mm
Wing Height	Vertical height of lower side wings	7.00 mm

E. Simulation Environment

The Time Domain Solver, which applies the Finite Integration Technique (FIT) for full-wave electromagnetic analysis, is used in CST Studio Suite to model and simulate the entire antenna structure, including the rook-shaped copper patch, FR-4 lossy substrate, and full copper ground plane. Because it calculates the broadband frequency response of the antenna from a single simulation run by stimulating the structure with a Gaussian pulse and computing the Fourier transform of the time-domain response, the Time Domain Solver is especially well suited for wideband antenna characterization. To precisely mimic the free-space radiation circumstances surrounding the antenna, the simulation boundary conditions are set up as open-add space. To excite the antenna and extract the S-parameters, VSWR, and far-field radiation patterns across the frequency range of 2 GHz to 3 GHz, which includes the target WLAN operating band, a discrete port is assigned at the base of the microstrip feed line. To ensure that simulation results converge to an accurate representation of the antenna's electromagnetic behavior, CST Studio Suite's adaptive meshing algorithm automatically refines the computational mesh in areas of high field gradient, such as the fine geometric features of the rook-shaped notches, the feed line junction, and the patch edges. Using the integrated far-field monitor, the far-field radiation pattern is calculated at the resonance frequency of 2.409 GHz, yielding three-dimensional gain and directivity distributions that describe the spatial radiation behavior of the suggested antenna.

III. Results and Discussion

CST Studio Suite was used to simulate the suggested rook-shaped microstrip patch antenna in the frequency range of 2 GHz to 3 GHz. This section presents and analyzes the simulated performance metrics, such as the S-parameter (return loss), Voltage Standing Wave Ratio (VSWR), and far-field radiation patterns. The findings verify that the antenna performs well at the target WLAN frequency of 2.4 GHz, displaying low reflected power, good impedance matching, and a distinct broadside radiation profile appropriate for WLAN communication.

A. S-Parameter Analysis

The main measure of how well the antenna absorbs power from the feed line at a particular frequency is the S-parameter, more precisely the reflection coefficient $S_{1,1}$. A significant amount of incident power is radiated rather than reflected back toward the source when the magnitude of $S_{1,1}$ is sufficiently negative in decibels at a specific frequency. $S_{1,1} \leq -10$ dB, or no more than 10% of the incident power being reflected at the antenna port, is the widely recognized threshold for practical antenna functioning. The excess negative margin provides tolerance against fabrication variations and environmental perturbations that may cause the resonant frequency to shift slightly from its simulated value. An antenna that exhibits return loss values significantly below this threshold is deemed well matched to its feed system.

Fig. 3 shows the simulated $S_{1,1}$ response of the suggested rook-shaped patch antenna. At 2.409 GHz, the curve shows a distinct resonance drop with a minimum return loss value of −18.831 dB. This number indicates a high degree of impedance matching between the 50 Ω feed line and the input impedance of the rook-shaped radiating patch at resonance, as it is about 8.831 dB below the typical −10 dB threshold. The narrow bandwidth feature commonly associated with single-layer microstrip patch antennas developed on moderately lossy substrates like FR-4 is consistent with the severity of the resonance dip. The suggested antenna is spectrally aligned with the target operating band since its resonance frequency of 2.409 GHz falls within the IEEE 802.11b/g/n WLAN channel allotment, which is centered at 2.412 GHz. The discretization of the rook-shaped geometry during mesh generation and the dispersive behavior of the FR-4 substrate at microwave frequencies are responsible for the small offset of 9 MHz from the nominal 2.4 GHz center frequency, which is within acceptable simulation tolerance. As would be predicted for a narrowband microstrip patch design, the $S_{1,1}$ curve returns to values near 0 dB outside the resonant band, indicating that the antenna does not radiate at frequencies distant from its resonance.

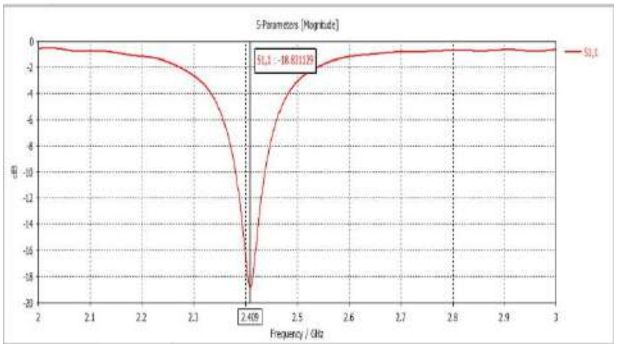

Fig. 3 Simulated $S_{1,1}$ response of the proposed antenna. Fig. 3. shows a resonance dip of −18.831 dB at 2.409 GHz in the simulated S-parameter ($S_{1,1}$) response of the suggested rook shaped microstrip patch antenna as a function of frequency from 2 GHz to 3 GHz.

B. VSWR Analysis

In terms of the ratio of maximum to minimum voltage amplitudes along the feed line, the Voltage Standing Wave Ratio is a complementary impedance matching metric that measures the degree of mismatch between the antenna input impedance and the characteristic impedance of the connecting transmission line. A VSWR of infinite denotes complete reflection, whereas a VSWR of 1.0 indicates a perfect impedance match with no reflected wave. The widely recognized standard for appropriate impedance matching in practical antenna applications is a VSWR value at or below 2.0 over the operating band, which translates to a return loss of roughly −9.54 dB and a reflected power fraction of almost eleven percent. In the physical prototype, achieving a VSWR far below 2.0 at the design frequency offers more protection against impedance drift brought on by adjacent objects, substrate tolerances, and connector parasitics.

Fig. 4 displays the suggested antenna's simulated VSWR response. The VSWR reaches a minimum value of 1.2583 at the resonant frequency of 2.409 GHz, which is much below the typical threshold of 2.0 and very close to the optimal value of unity. This result verifies that the rook-shaped patch is well matched to the 50 Ω feed line at its resonance frequency, with little signal reflection at the antenna port, and supports the return loss observation shown in Fig. 3. The VSWR curve traces a valley profile typical of a single resonant mode, falling sharply from high values at frequencies below 2.3 GHz, reaching its minimum at 2.409 GHz, and then rising once again toward higher values above 2.5 GHz.

The antenna's acceptable impedance bandwidth for WLAN operation is determined by the frequency range over which the VSWR curve stays below the 2.0 threshold. The design's single-layer, single-patch architecture and the FR-4 substrate's moderate permittivity are compatible with the narrow bandwidth profile. The suggested rook-shaped antenna provides excellent impedance matching at the 2.4 GHz WLAN band, as demonstrated by the VSWR result and the S-parameter analysis.

The suggested rook-shaped microstrip patch antenna's simulated voltage standing wave ratio (VSWR) over the frequency range of 2 GHz to 3 GHz is shown in Fig. 4, with a minimum VSWR of 1.2583 at 2.409 GHz.

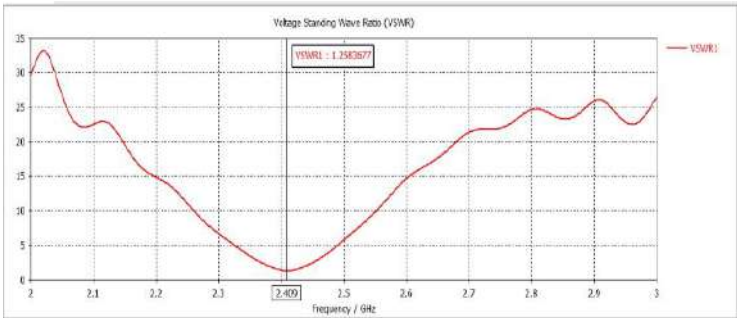

Fig. 4 Simulated VSWR of the proposed antenna

C. Radiation Pattern Analysis

An antenna's spatial distribution of electromagnetic power as a function of direction in three-dimensional space is described by its radiation pattern. A broadside radiation pattern, where the maximum radiated power is directed perpendicular to the antenna's plane, is typically preferred for WLAN applications because it enables the antenna to efficiently communicate with devices situated above or in front of the host device's surface. Due to the constructive interference of fields radiated from the two radiating edges of the patch, which are separated by about half a guided wavelength and radiate in phase in the broadside direction, microstrip patch antennas naturally have a tendency to display broadside radiation.

Two complementary perspectives of the simulated far-field radiation pattern of the suggested rook-shaped microstrip patch antenna at the resonance frequency of 2.409 GHz are shown. Looking down along the axis perpendicular to the patch surface, Fig. 5 depicts the top view of the three-dimensional radiation pattern. The radiation pattern's three-dimensional perspective view is shown in Fig. 6, giving a comprehensive view of the spatial power distribution around the antenna.

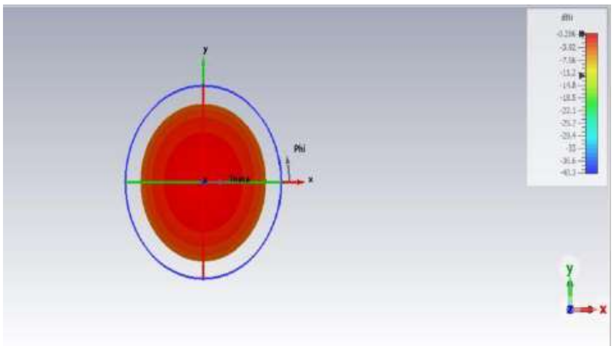

Fig. 5 Top view of the far-field radiation pattern

With a peak gain of −0.286 dBi, the top view of the simulated three-dimensional far-field radiation pattern of the suggested rook-shaped microstrip patch antenna at 2.409 GHz illustrates the near-omnidirectional azimuthal characteristic when viewed along the broadside axis.

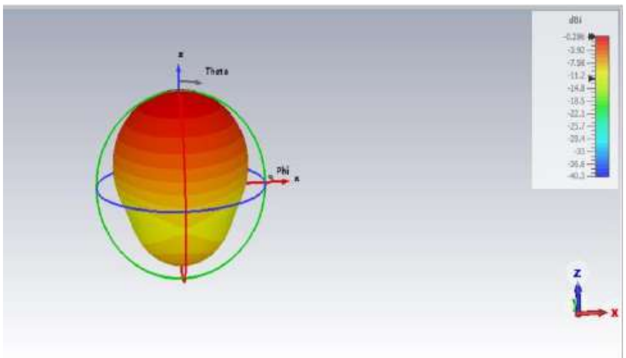

Fig. 6 3D view of the far-field radiation pattern

Fig. 6. shows a three-dimensional perspective image of the simulated far-field radiation pattern of the suggested rook-shaped microstrip patch antenna at 2.409 GHz. It shows the reduced back radiation below the ground plane and the broadside radiation lobe pointing upward along the positive z-axis.

The antenna radiates with a near-omnidirectional characteristic when viewed from above, as shown by the top view of the radiation pattern in Fig. 5, which shows a nearly circular and uniform distribution of radiated power in the azimuthal plane. The rook-shaped patch's fourfold symmetric geometry, which uniformly distributes the radiating edge fields over the patch's perimeter and inhibits the development of large preferential azimuthal lobes, is directly responsible for this azimuthal uniformity. This feature is especially useful for WLAN applications, where the antenna must maintain constant link quality independent of the azimuthal angle of arrival and the orientation of the communication device with respect to the access point or router is typically unknown.

The height characteristics of the radiation pattern are further explained by the three-dimensional perspective image shown in Fig. 6. The expected broadside behavior of the microstrip patch antenna structure is confirmed by the dominating radiation lobe's unambiguous direction along the positive z-axis, which is perpendicular to the patch's plane. The gain progressively decreases as the observation angle shifts from the broadside direction toward the horizon, and the lobe shape is hemispherical and gently tapered. The back radiation that travels through the ground plane and the finite-thickness FR-4 substrate is represented by a smaller secondary lobe that can be seen beneath the ground plane. This back lobe is a well-known feature of microstrip patch antennas with finite ground planes, and it is more noticeable when lossy substrates are employed because the substrate losses lessen the ground plane's ability to shelter the antenna structure's edges.

The antenna's peak realized gain, measured in the broadside direction at the resonant frequency of 2.409 GHz, is −0.286 dBi. Although this gain value is small in absolute terms, it is in line with the anticipated performance of a single-element microstrip patch antenna installed on a FR-4 lossy substrate, where conductor losses in the copper layers and dielectric losses in the substrate result in a lower radiation efficiency than would be attained on a low-loss microwave substrate. Future revisions of the device could increase the gain by using a lower-loss substrate in place of FR-4, adding a bigger reflector ground plane, or setting up several rook-shaped patch elements in a phased array configuration to increase directivity. The proposed antenna's overall radiation behavior, which includes broadside gain, azimuthal symmetry, and a clearly defined main lobe, validates its appropriateness for deployment in 2.4 GHz WLAN systems where upward broadside radiation and omnidirectional horizontal coverage are both operationally beneficial.

IV.CONCLUSION

The design and electromagnetic simulation of a rook-shaped microstrip patch antenna meant to function in the 2.4 GHz WLAN band were given in this research. The radiating patch and ground plane of the antenna were made of annealed copper on a FR-4 lossy dielectric substrate with a relative permittivity of 4.4 and a loss tangent of 0.02. Inspired by the battlement profile of the rook chess piece, the unique rook-shaped geometry was achieved by introducing a periodic arrangement of uniform rectangular notches along all four sides of a conventionally dimensioned rectangular patch. By extending the effective surface current path length across the radiating element, this boundary modification shifted the fundamental resonance toward the target frequency without increasing the antenna's overall physical footprint or adding more matching circuitry. The rook shape was then parameterized and improved using full-wave simulation in CST Studio Suite using the Finite Integration Technique after the initial patch dimensions were determined analytically using the transmission line model. The antenna was excited using an edge feeding setup with a 50 Ω microstrip line, which provides a simple and fabrication-friendly feed configuration without the need for via-hole connections or aperture coupling devices.

With a return loss of −18.831 dB and a VSWR of 1.2583, the simulation results verified resonance at 2.409 GHz, both of which easily meet the typical performance limits for realistic antenna deployment in wireless communication systems. With a primary lobe oriented perpendicular to the patch surface and a nearly omnidirectional distribution in the azimuthal plane, the far-field radiation pattern at the resonant frequency demonstrated a distinct broadside characteristic, resulting in a peak gain of −0.286 dBi. Together, these findings demonstrate that the rook-shaped border modification effectively directs the patch's resonant behavior toward the intended operating frequency while maintaining the essential radiation characteristics connected to microstrip patch antenna topologies. Geometrically motivated patch shaping, a common low-cost substrate material, and a straightforward feeding mechanism show that intentional geometric design, as opposed to material complexity or circuit-level matching networks, can achieve significant impedance matching performance at 2.4 GHz. The suggested antenna can be easily integrated into WLAN-capable consumer electronics, embedded wireless modules, and Internet of Things end devices because it is small, planar, and completely compatible with standard PCB fabrication procedures.

In order to verify the simulated results against measured data, future work will concentrate on the physical fabrication of the proposed antenna using standard PCB etching processes, followed by experimental characterization using a vector network analyzer and an anechoic chamber measurement setup. Further research will examine the impact of ground plane size variation on radiation efficiency and back lobe suppression, the possibility of bandwidth enhancement through the introduction of a partial ground plane or parasitic patch elements, and the adaptation of the rook geometry to dual-band or wideband operation by adding multi-scale notch configurations with different depth and periodicity.

REFERENCES

[1] Balanis, *Antenna Theory: Analysis and Design*, 4th ed. Hoboken, NJ, USA: Wiley, 2016.

[2] IEEE Standard for Information Technology-Telecommunications and Information Exchange Between Systems-Local and Metropolitan Area Networks—Specific Requirements Part 11: Wireless LAN Medium Access Control (MAC) and Physical Layer (PHY) Specifications, IEEE Std 802.11n-2009, 2009.

[3] D. M. Pozar, "Microstrip antenna aperture-coupled to a microstripline," *Electronics Letters*, vol. 21, no. 2, pp. 49–50, Jan. 1985.

[4] R. Garg, P. Bhartia, I. Bahl, and A. Ittipiboon, *Microstrip Antenna Design Handbook*. Norwood, MA, USA: Artech House, 2001.

[5] K. L. Wong, *Compact and Broadband Microstrip Antennas*. New York, NY, USA: Wiley, 2002.

[6] S. Maci and G. B. Gentili, "Dual-frequency patch antennas," *IEEE Antennas and Propagation Magazine*, vol. 39, no. 6, pp. 13–20, Dec. 1997.

[7] A. A. Deshmukh and G. Kumar, "Compact broadband U-slot loaded rectangular microstrip antennas," *Microwave and Optical Technology Letters*, vol. 46, no. 6, pp. 556–559, Sep. 2005.

[8] C. Puente-Baliarda, J. Romeu, R. Pous, and A. Cardama, "On the behavior of the Sierpinski multiband fractal antenna," *IEEE Transactions on Antennas and Propagation*, vol. 46, no. 4, pp. 517–524, Apr. 1998.

[9] J. Anguera, C. Puente, C. Borja, and J. Soler, "Fractal shaped antennas: A review," in *Encyclopedia of RF and Microwave Engineering*, K. Chang, Ed. Hoboken, NJ, USA: Wiley, 2005, pp. 1620–1635.

[10] F. Falcone, T. Lopetegi, J. D. Baena, R. Marques, F. Martin, and M. Sorolla, "Effective negative-ε stopband microstrip lines based on complementary split ring resonators," *IEEE Microwave and Wireless Components Letters*, vol. 14, no. 6, pp. 280–282, Jun. 2004.

[11] Y. X. Guo, K. M. Luk, and K. F. Lee, "L-shaped probe fed thick-substrate patch antennas for dual-band operation," *IEEE Transactions on Antennas and Propagation*, vol. 51, no. 8, pp. 1986–1991, Aug. 2003.

[12] G. Bharadwaj, S. Chandel, and A. K. Shankhwar, "Design of geometrically shaped microstrip patch antenna for wireless communication applications," *International Journal of Electronics and Communications*, vol. 93, pp. 316–323, Aug. 2018.

[13] CST Studio Suite 2023 User Manual, Dassault Systèmes, Vélizy-Villacoublay, France, 2023.

[14] I. J. Bahl and P. Trivedi, "A designer's guide to microstrip line," *Microwaves*, vol. 16, no. 5, pp. 174–182,

[15] May 1977.

[16] M. Clemens and T. Weiland, "Discrete electromagnetism with the finite integration technique," *Progress in Electromagnetics Research*, vol. 32, pp. 65–87, 2001.

[17] W. L. Stutzman and G. A. Thiele, *Antenna Theory and Design*, 3rd ed. Hoboken, NJ, USA: Wiley, 2012.